Global signal topography in the human brain differs systematically across the lifespan

Jason S. Nomi[1*], Danilo Bzdok[2,3*], Jingwei Li[4], Taylor Bolt[1,5], Salome Kornfeld[6], Zachary T. Goodman[7], B.T. Thomas Yeo[4], R. Nathan Spreng,[3,8,9], & Lucina Q. Uddin[1,10]

[1]Department of Psychiatry and Biobehavioral Sciences, University of California Los Angeles, CA, USA

[2]Department of Biomedical Engineering, Montreal Neurological Institute (MNI), Mila - Quebec Artificial Intelligence Institute, Quebec, Canada

[3]Brain-imaging institute (BIC), McGill University, Montreal, QC, Canada;

[4]Electrical and Computer Engineering, Centre for Sleep & Cognition, Centre for Translational MR Research, N.1 Institute for Health & Institute for Digital Medicine, National University of Singapore, Singapore

[5]Deloitte, People Analytics, Atlanta, GA, USA

[6]REHAB Basel, Klinik fur Neurorehabmilitation und Paraplegiologie, Basel, Switzerland

[7]Department of Psychology, University of Miami, Coral Gables, FL, USA

[8]Laboratory of Brain and Cognition, Montreal Neurological Institute, Department of Neurology and Neurosurgery, McGill University, Montreal, QC, Canada

[9]Departments of Psychiatry and Psychology, McGill University, Montreal, QC, Canada

[10]Department of Psychology, University of California Los Angeles, CA, USA

*These authors contributed equally

Correspondence should be addressed to:

Jason S. Nomi
University of California Los Angeles
Semel Institute for Neuroscience and Human Behavior
Email: JNomi@mednet.ucla.edu

Lucina Q. Uddin
University of California Los Angeles
Semel Institute for Neuroscience and Human Behavior
Email: lucina@ucla.edu

Abstract

Global signal regression effectively mitigates noise in fMRI data but also inadvertently removes neural signals of interest. We show distinct linear and quadratic lifespan global signal topography associations with age. We also show that global signal regression significantly influences age-functional connectivity strength associations. These findings have critical implications for lifespan network neuroscience investigations, given that a widely-used data denoising step differentially impacts brain connectivity effects in different age cohorts.

Keywords: aging, artifact removal, brain development, denoising strategies, intrinsic functional connectivity, frontoparietal network, signal versus noise, population neuroscience

One of the biggest challenges in neuroscience is separating signal from noise (1). In functional neuroimaging generally, and in human connectomics investigations utilizing resting state functional MRI (fMRI) specifically, this challenge has been met with the development of processing pipelines that mitigate artifacts known to obscure the underlying neural signal (2). These pipelines denoise fMRI data by removing physiological, hardware-related, and head motion-related signals to identify functional network architectures in the human brain. The "global signal" constitutes the average signal intensity across all voxels in the brain (generally gray matter, but can include non-gray matter). Global signal regression has been widely adopted as a robust method for attenuating cardiac and respiratory noise and other non-random confounding signals (2) and has also been shown to improve prediction of behavior from functional connectivity (FC) indices in certain scenarios (4). However, the benefits from global signal regression may come at the expense of removing neural signals of interest.

Several lines of emerging evidence suggest a cautious approach is warranted when exercising what is sometimes viewed as an aggressive data cleaning strategy. This is because the global signal also includes important neural activity. Animal studies show that the fMRI global blood-oxygen level-dependent (BOLD) signal is strongly associated with neuronal activity using photometry imaging of neurons (5) and intracranial electrical recordings (6). These physiological associations between the global signal and electrical activity may be rich sources of individual differences in cognition and behavior. Recently, we identified a dynamic spatiotemporal pattern explaining ~20% of resting-state BOLD variance that has a time series strongly associated (r = 0.97) with the global signal in adult humans (7). This suggests that the global signal facilitates the propagation of cortex wide activity across brain networks encompassing a substantial portion of spontaneous brain function. We have also shown that global signal topography, or the association between each voxel's time series and the global signal, contains information related to trait-level cognition and behavior. In a population neuroscience study of >1000 subjects, global signal topography was related to an axis of positive and negative life outcomes and psychological function, particularly weighted in frontoparietal executive control network regions, in 22-37 year-old adults (8). These studies suggest a significant neural component of the global signal related to individual physiological and cognitive differences; it is not solely a source of pure noise to be discarded.

These observations invigorate the claim that the global signal potentially has relevance for lifespan studies of the human connectome. In prior network neuroscience research, the question of how global signal topography varies with age has not been carefully considered. Consequently, existing findings documenting lifespan changes in FC influenced by global signal regression would need to be revisited to determine how such results were impacted on a systems-wide basis. Thus, understanding the impact of global signal regression is important for interpreting both past and future studies focusing on age or lifespan FC associations.

Using a large cross-sectional sample (601 subjects; 6-86 years old; 10 minute resting-state fMRI scan) of publicly available data (NKI-enhanced; **Figure 1**), we demonstrate distinct linear and quadratic associations between global signal topography and age for the first time. To mitigate head motion concerns, all participants had an average framewise displacement (FD) < 0.5 mm, high motion frames were censored (3) (FD > 0.5 mm), and FD was included as a covariate in all regression models (there was an age x FD linear interaction ($p < 0.001$) but no quadratic interaction ($p = 0.9$)). The thalamus and higher-level visual cortices show a positive linear relationship, where the association with the global signal is weakest for younger individuals and strongest for older individuals. Temporal cortex and sensorimotor areas show

the opposite pattern, where the association with the global signal is strongest for younger individuals and weakest for older individuals (**Figure 2**). The lateral frontoparietal network has a quadratic association with the global signal; these regions show stronger associations at early (< 20 years) and later (> 60 years) periods of life, and the weakest association in middle age. The opposite pattern emerges in the medial prefrontal cortex, caudate, and lower-level visual cortices, where the association with the global signal is weakest at early and later periods of life, and strongest in middle age. These results demonstrate distinct age-dependent large-scale network associations with the global signal.

It is currently unclear to what extent these brain system-specific lifespan global signal spatial topographies are driven by vascular or neural properties within the context of the current study. Evidence for a neural origin related to the current results come from developmental trajectories of brain network composition and executive function behavioral performance. Functional connections typically show a curvilinear pattern of network development; long-distance within-network connections strengthen and between-network connections segregate into the 3rd and 4th decade of life (9). The opposite pattern continues into old age, where between-network integration and within-network segregation increase (10, 11, 12). The FC strength of nodes within the lateral frontoparietal network closely resembles executive function performance across the lifespan (13). That is, FC strength within nodes of the frontoparietal network is strongest when executive function performance is highest and within-network connectivity strength is weakest when executive function performance is lowest across the lifespan. These lifespan changes in network integration and segregation that mirror executive function behavioral performance, both show a similar quadratic relationship as the association between the frontoparietal network and the global signal in the current study. These findings suggest an association between the global signal spatial topography changes observed in the current results with known lifespan characterizations of brain network and behavioral changes.

Evidence for a vascular origin of the global signal related to the current results come from research orthogonalizing CO2 and stimulus presentation showing that the lateral frontoparietal, medial frontoparietal, and visual networks have dissociable vascular and neural fMRI BOLD activity within a task paradigm (14). Additional fMRI research shows that vascular effects of aging can also be both global and brain region dependent (15). Thus, it may be possible that this divergence among large scale network global signal topography is driven by such vascular processes or the previously described executive function performance association with the frontoparietal network. It is not possible to disentangle the two within the current study, but the differentiation of global signal lifespan topography in a network specific manner is an important consideration for the judicious application of global signal regression in future studies.

Accordingly, we also show that the processing step of global signal regression has a significant influence on the amount and magnitude of linear and quadratic FC associations with age (**Figure 3**). Negative linear effects for between-network connections related to the default mode network (DMN) are drastically reduced, with some negative within-network DMN effects turning into positive linear effects. Additionally, within- and between-network connections related to the sensorimotor and visual networks are strengthened, and the frontoparietal network shows stronger negative linear effects with the sensorimotor and visual networks. Quadratic effects related to global signal regression show a general increase in the number of within- and between-network connections for the DMN and ventral attention networks. Thus, global signal

regression exerts a strong influence on both linear and quadratic FC-age associations on both within- and between-network connections across the lifespan.

The changing global signal topography across the lifespan and the influence of global signal regression on age-FC associations makes interpretation of lifespan studies using global signal regression complex. As the sample age-range increases, there is a greater possibility that different brain areas and networks will be influenced. For example, global signal regression may have a greater influence on the frontoparietal network in child and older adult samples compared with young adult samples. Additionally, global signal regression applied to data collected from young individuals may not influence thalamic and occipital cortex activity as much as global signal regression applied to older adults. Thus, global signal regression may have system-specific implications in age-FC investigations. Further, it is unknown to what extent global signal regression is beneficial or detrimental for identifying cognition-related brain activity. It is not possible to determine if the global signal is driving activity in specific networks, or vice-versa. Regardless, consideration of how global signal regression influences lifespan results are warranted, as even the physiological component of the global signal is a rich source of individual differences in brain function (7).

In sum, we show that age is strongly associated with the spatial topography of the global signal in resting-state fMRI data. Due to the importance and controversy over global signal regression, researchers should take care to consider the implications of its application beyond artifact mitigation. As the field of fMRI marches forward, understanding how global signal regression affects statistical analyses will continue to be of paramount importance for lifespan network neuroscience investigations.

Figure 1: Demographic information and average global signal topography across randomly chosen age groups. **Left:** Histograms of age, scatterplots showing significant linear age-framewise displacement (FD) associations, and pie charts of sex distribution. There is a significant linear age x FD interaction ($p < 0.001$) but not a quadratic age x FD interaction ($p = 0.9$) **Right:** Average global signal spatial topography across every 10 years of the lifespan. The strongest associations are present in the occipital and lateral frontal brain areas. The global signal topography matches previous research showing strong associations between the global signal and visual areas (Li et al., 2019; Bolt et al., In Press) as well as frontoparietal areas (Zhang et al., 2019; Li et al., 2020) across all age groups showing that average global signal topography is relatively stable across the lifespan.

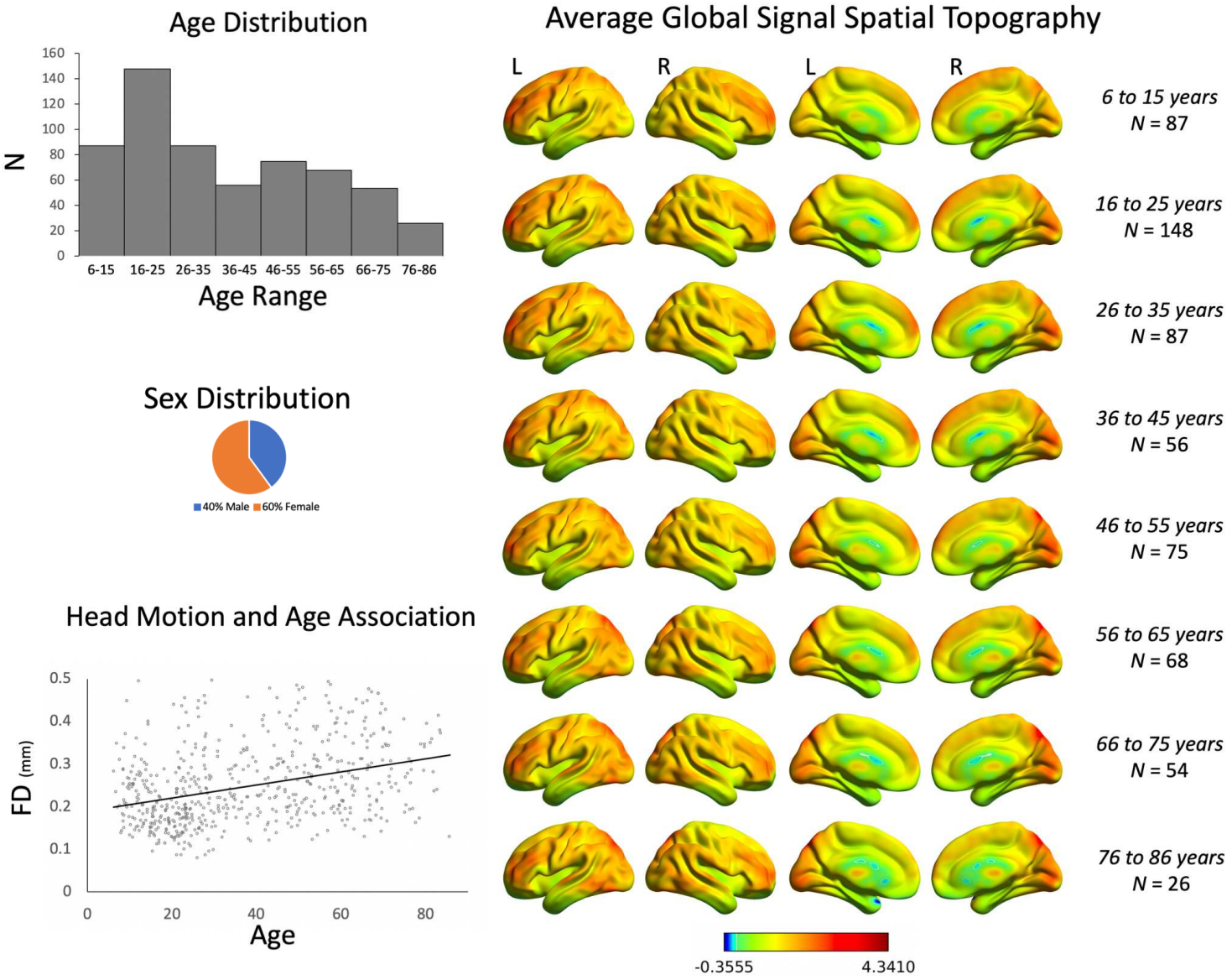

Figure 2: Linear and quadratic associations between the global signal and voxel-wise time-series. Each dot denotes an individual subject's z-scored unstandardized beta representing the association between the global signal and each cluster's average time series across its constituent voxels. **Top Left**: Positive linear associations were present in the thalamus, occipital, and parietal cortices. **Top Right**: Positive quadratic associations were present across nodes of the frontoparietal network, frontal eye fields, and putamen. **Bottom Left**: Negative linear associations were present in the medial prefrontal cortex, sensorimotor, temporal cortex, frontal cortex, and basal ganglia. **Bottom Right**: Negative quadratic associations were present in the medial prefrontal cortex, occipital cortex, and the caudate. These differences in global signal topography according to age and network suggest that global signal regression may have a systematic influence on networks according to age.

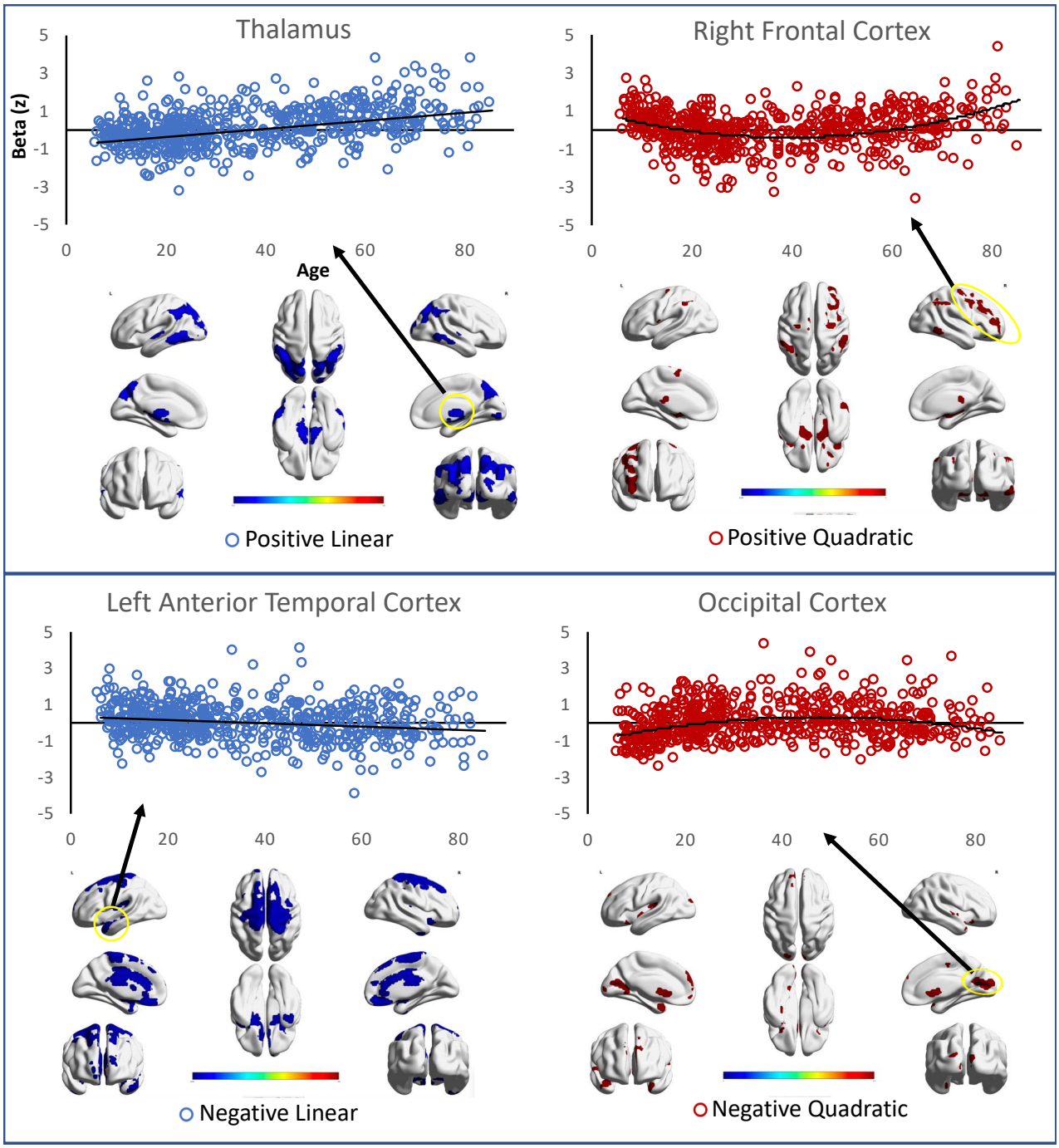

Figure 3: **Influence of global signal regression on Age-FC strength and amount of significant connections.** Linear and quadratic unstandardized betas representing the association between functional connectivity strength and age with and without global signal regression for the 400 ROI Schaefer Parcellation. Warm colors indicate larger unstandardized betas (stronger associations) and cool colors indicate smaller unstandardized betas (weaker associations) for connections surviving FDR correction ($q < 0.001$). White indicates connections not surviving FDR correction. DA = dorsal attention network; VA = ventral attention network; SM = sensorimotor network. Global signal regression results in stronger linear effects for visual-sensorimotor connections, weaker linear effects for within- and between-network default mode connections, and weaker connections between the frontoparietal control network and visual-sensorimotor areas. Global signal regression also results in more negative quadratic betas for connections within the ventral attention network, sensorimotor network, and default mode network in addition to more negative quadratic betas between the dorsal and ventral attention networks.

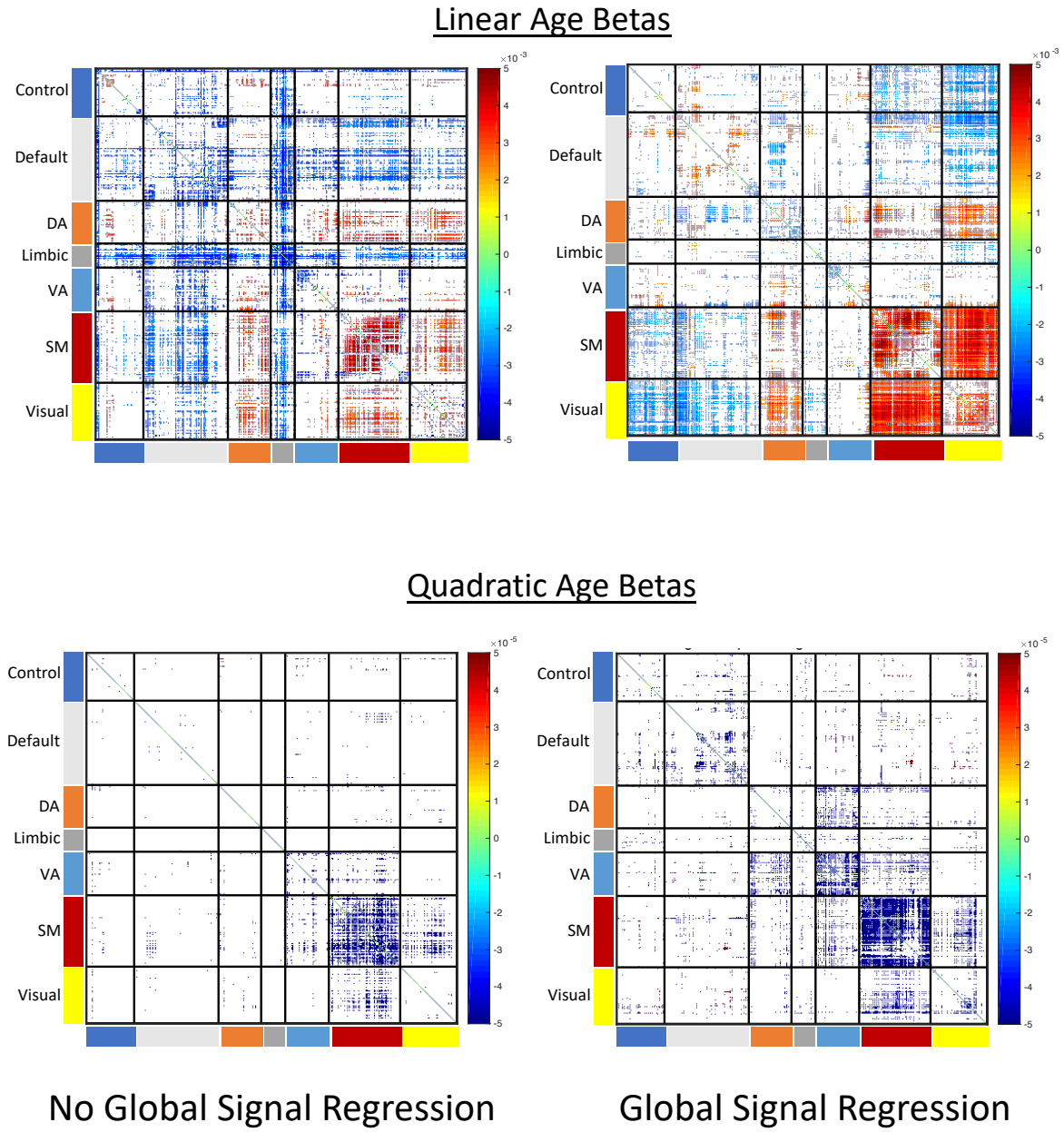

References

1) Uddin, L. Q. (2020). *Trends in Cognitive Sciences*, *24*(9), 734-746.

2) Ciric, R., Rosen, A.F., Erus, G., Cieslak, M., Adebimpe, A., Cook, P.A., Bassett, D.S., Davatzikos, C., Wolf, D.H. and Satterthwaite, T.D., 2018. *Nature protocols*, *13*(12), pp.2801-2826.

3) Power, J.D., Barnes, K.A., Snyder, A.Z., Schlaggar, B.L. and Petersen, S.E., 2012. *Neuroimage*, *59*(3), pp.2142-2154.

4) Li, J., Kong, R., Liégeois, R., Orban, C., Tan, Y., Sun, N., Holmes, A.J., Sabuncu, M.R., Ge, T. and Yeo, B.T., 2019. *NeuroImage*, *196*, pp.126-141

5) Ma, Y., Ma, Z., Liang, Z., Neuberger, T. and Zhang, N., 2020. *Brain Structure and Function*, *225*(1), pp.227-240.

6) Schölvinck, M.L., Maier, A., Ye, F.Q., Duyn, J.H. and Leopold, D.A., 2010. *Proceedings of the National Academy of Sciences*, *107*(22), pp.10238-10243.

7) Bolt, T., Nomi, J.S., Bzdok, D., Chang, C., Yeo, B.T., Uddin, L.Q., and Kielholz, S.D. (2022) *Nature Neuroscience*.

8) Li, J., Bolt, T., Bzdok, D., Nomi, J.S., Yeo, B.T., Spreng, R.N. and Uddin, L.Q., 2019. *Scientific reports*, *9*(1), pp.1-10.

9) Fair, D.A., Cohen, A.L., Power, J.D., Dosenbach, N.U., Church, J.A., Miezin, F.M., Schlaggar, B.L. and Petersen, S.E., 2009. *PLoS computational biology*, *5*(5), p.e1000381.

10) Vij, S.G., Nomi, J.S., Dajani, D.R. and Uddin, L.Q., 2018. *Neuroimage*, *173*, pp.498-508.

11) Zuo, X.N., He, Y., Betzel, R.F., Colcombe, S., Sporns, O. and Milham, M.P., 2017. *Trends in cognitive sciences*, *21*(1), pp.32-45.

12) Setton, R., Mwilambwe-Tshilobo, L., Girn, M., Lockrow, A.W., Baracchini, G., Hughes, C., Lowe, A.J., Cassidy, B.N., Li, J., Luh, W-M., Bzdok, D., Leah, R.M., Ge, T., Margulies, D.S., Music, B., Bernhardt, B.C., Stevens, W.D., De Brigard, Fl., Kund, P., Turner, G.R., Spreng, R.N. (2022) *Cerebral Cortex*.

13) Ferguson, H.J., Brunsdon, V.E. and Bradford, E.E., 2021. *Scientific reports*, *11*(1), pp.1-17.

14) Bright, M.G., Whittaker, J.R., Driver, I.D. and Murphy, K., 2020. *NeuroImage*, *217*, p.116907.

15) Tsvetanov, K.A., Henson, R.N., Jones, P.S., Mutsaerts, H., Fuhrmann, D., Tyler, L.K., Cam-CAN and Rowe, J.B., 2021. *Psychophysiology*, *58*(7), p.e13714.

Online Materials and Methods

Subjects and fMRI data

A 10-minute resting-state scan (TR = 1.4 sec, 10 minutes) was analyzed for six hundred and one subjects (6-85 years old; 240 males) without a current DSM diagnosis from the Nathan Kline Institute enhanced publicly available data repository (1). All participants had an average framewise displacement < 0.5 mm. Imaging was performed on a Siemens Trio 3.0T scanner that collected a T1 anatomical image and multiband (factor of 4) EPI sequenced resting-state fMRI data (2x2x2 mm, 40 interleaved slices, TR = 1.4s, TE = 30 ms, flip angle = 65°, FOV = 224 mm, 404 volumes). Participants were instructed to keep their eyes open and fixate on a cross centered on the screen (http://fcon_1000.projects.nitrc. org/indi/enhanced/mri_protocol.html). All participants had less than 0.5 mm average framewise displacement (FD). There was a significant linear FD-age association (standardized $\beta = 0.35$, $p = 1.23E\text{-}18$) but no quadratic FD-age association ($p = 0.9$) (**Figure 1**). Therefore, FD was used as a nuisance covariate in all analyses.

fMRI preprocessing

Data were preprocessed using FSL, AFNI, and SPM functions through DPARSF-A in DPABI (2). The first five images were removed to allow the MRI signal to reach equilibrium. Data were despiked using AFNI 3dDespike, realigned and normalized with DPARSF-A into 3mm MNI space, and then smoothed (6mm FWHM). The ICA-FIX classifier (3, 4) was trained on hand-classified independent components separated into noise and non-noise categories (random sampling by choosing subjects separated by ~10 years of age) by visual inspection. The resulting component classifications were then fed into the ICA-FIX classification algorithm to classify noise and non-noise components from individual subject data before conducting nuisance regression of classified noise components from the resting-state scans in MNI space. Next, the Friston 24 motion parameters and linear trends were regressed out of the data, before the application of a band-pass filter (0.01 to .10 Hz) to isolate low-frequency fluctuations that characterize resting-state BOLD signals.

Global Signal Topography and the General Linear Model

The global signal was calculated as the mean time-series of all gray matter voxels within a SPM gray matter a priori mask. The association between the global signal time series and the time series at each voxel was calculated using linear regression and produced whole-brain voxel-wise beta maps for each subject. Frames where FD (5) exceeded 0.5 mm were not included in the regression model. The whole-brain voxel-wise subject maps were then smoothed (6mm FWHM). Two general linear models (GLM) were then run in FSL using whole-brain voxel-wise beta maps as the DVs. IVs for the first GLM consisted of linear age, mean FD, and sex, and the IVs for the second GLM consisted of linear age, quadratic age, mean FD, and sex.

Influence of Global Signal Regression on Network Node Association Strength Across the lifespan

In order to determine how global signal regression influences the association between age and FC strength between two network nodes, two regression models were run on data with and without global signal regression. The DVs for both regression models were the within-subject z-transformed Pearson correlation matrix for each pair of ROI time series in the Schaefer parcellation (400 ROIs: (6)). The first model consisted of age, FD, and sex as IVs while the second model used age, age squared, FD, and sex as IVs (FDR corrected $q < 0.001$).

References

1) Nooner, K.B., Colcombe, S.J., Tobe, R.H., Mennes, M., Benedict, M.M., Moreno, A.L., Panek, L.J., Brown, S., Zavitz, S.T., Li, Q. and Sikka, S., 2012. The NKI-Rockland sample: a model for accelerating the pace of discovery science in psychiatry. *Frontiers in neuroscience*, *6*, p.152.

2) Yan, C.G., Wang, X.D., Zuo, X.N. and Zang, Y.F., 2016. DPABI: data processing & analysis for (resting-state) brain imaging. *Neuroinformatics*, *14*(3), pp.339-351.

3) Griffanti, L., Salimi-Khorshidi, G., Beckmann, C.F., Auerbach, E.J., Douaud, G., Sexton, C.E., Zsoldos, E., Ebmeier, K.P., Filippini, N., Mackay, C.E. and Moeller, S., 2014. ICA-based artefact removal and accelerated fMRI acquisition for improved resting state network imaging. *Neuroimage*, *95*, pp.232-247.

4) Salimi-Khorshidi, G., Douaud, G., Beckmann, C.F., Glasser, M.F., Griffanti, L. and Smith, S.M., 2014. Automatic denoising of functional MRI data: combining independent component analysis and hierarchical fusion of classifiers. *Neuroimage*, *90*, pp.449-468.

5) Power, J.D., Barnes, K.A., Snyder, A.Z., Schlaggar, B.L. and Petersen, S.E., 2012. *Neuroimage*, *59*(3), pp.2142-2154.

6) Schaefer, A., Kong, R., Gordon, E.M., Laumann, T.O., Zuo, X.N., Holmes, A.J., Eickhoff, S.B. and Yeo, B.T., 2018. Local-global parcellation of the human cerebral cortex from intrinsic functional connectivity MRI. *Cerebral cortex*, *28*(9), pp.3095-3114.